Design of a Tri-Band Printed Monopole Antenna for WLAN and GPS Applications

[#]Jynu-Yu Zou [1], Cheng-Hsun Wu [1], Tzyh-Ghuang Ma [1]
[1] Department of Electrical Engineering, National Taiwan University of Science and Technology
No. 43, Keelung Rd. Sec. 4, Taipei 10607, Taiwan (R.O.C.), e-mail: M9907618@mail.ntust.edu.tw; D9907604@mail.ntust.edu.tw; tgma@mail.ntust.edu.tw

Abstract

In this paper, a printed monopole antenna for tri-band operation is presented. The proposed antenna is comprised of a T-shape monopole, a rectangular ring, two spiral lines, and a trapezoidal metal plate. It has an overall size of 40 × 41.2 × 0.508 mm^3 with three resonance frequencies at 1.575, 2.4, and 5.2 GHz.

Keywords : Tri-band, T-shape monopole, Wireless local area network, Global positioning system.

1. Introduction

The wireless communication has experienced a huge evolution in the past decade. A variety of protocols, such as the wireless local area network (WLAN) and the global positioning system (GPS), have become the standard facilities on the portable devices. To maintain an overall compact size while cover a number of systems with different operating frequencies, a compact antenna capable of multi-band operation would be necessarily required [1]-[7]. Design examples include the stacked antennas [1]-[3], the dielectrically-loaded antenna [4], the right/left-handed antenna [5], the cavity-backed slot antenna [6], and the slot antenna on the high impedance surface [7]. While the stacked antennas [1]-[3] and the cavity-backed slot antenna [6] need multilayer fabrication process, the dielectrically-loaded antenna [4] is complicated in structure. The antennas in [5] and [7], in the meantime, require via holes and hence increase the overall cost.

In this paper, we propose a tri-band printed monopole antenna, which covers the IEEE 802.11a/b/g/n standards at the 2.4-GHz (2400-2484 MHz) and 5-GHz (5150-5850 MHz) bands; it operates at the GPS L1 band at 1.575 GHz, as well. The proposed antenna features a simple structure with a low-cost via-free manufacturing process. The radiation patterns, in the meantime, show fairly omnidirectional patterns at all three resonance frequencies. Details of the antenna design and the simulated and experimental results are presented and discussed in the following sections.

2. Antenna Configuration and Design Guidelines

The geometry of the proposed antenna is shown in Fig. 1 along with the design parameters. In this study, the Roger RO4003C substrate, with a thickness of 0.508 mm, relative dielectric constant of 3.38, and loss tangent of 0.0027, was used. The antenna consists of a T-shape radiator, a rectangular ring, a pair of spiral lines, and a trapezoidal metal plate. The trapezoidal plate helps obtain good impedance matching, while all other components are designed to achieve three resonance modes at the designate frequency bands.

The simulated current distributions on the antenna surface at 1.575, 2.4, and 5.2 GHz are shown in Fig. 2(a), (b), and (c). At 1.575 and 5.2 GHz, the current is mainly concentrated on the Path 1, which consists of the T-shape radiator with the rectangular ring inserted. On the other hand, the surface current at 2.4-GHz is mainly distributed along the Path 2, i.e. the two spiral lines. It is worthy to mention that although the currents in the 1.575- and 5.2-GHz bands share the same resonating path, the equivalent electrical length is about $3\lambda_g/4$ in the high band and becomes $\lambda_g/4$ in the lower one.

The parameters (L_2, L_3, and W_4) can be controlled to achieve the desired tri-band operations. Fig. 3(a), (b), and (c) shows the $|S_{11}|$ responses versus frequencies with different sets of

parametric studies. It is obvious that the Path 1 is dependent on the length L_2, which, in turn, determines the antenna resonance frequencies at the GPS and 5-GHz WLAN bands. The length L_3 dominates the resonance of the 2.4-GHz WLAN band; it also affects the impedance matching of the other bands, as the Path 2 actually appears as an impedance loading on the Path 1. In addition, the resonance mode for the 5-GHz band can be also controlled by the length W_4, as indicated in Fig. 3(c); it, however, has limited effects on the resonance at the GPS band. Finally, as shown in Fig. 3(d), the slot ($S_1 \times S_2$) in the trapezoidal metal plate is a half-wave resonator, which is used to block away the unwanted spectra around 6.9 GHz without any loss of performance within the three operation bands (1.575, 2.4, and 5.2 GHz). With the parametric analysis, the proposed antenna can be optimized to achieve the required performance.

3. Simulation and Experimental Results

By utilizing the design guidelines in Sec. 2, the final parameters of the antenna are $W_1 = 21$ mm, $W_2 = 1.5$ mm, $W_3 = 0.5$ mm, $W_4 = 3.8$ mm, $W_5 = 0.8$ mm, $W_6 = 21.1$ mm, $W_7 = 6$ mm, $W_8 = 1.1$ mm, $W_9 = 41.2$ mm, $S_1 = 0.4$ mm, $S_2 = 16$ mm, $L_1 = 13.5$ mm, $L_2 = 9$ mm, $L_3 = 7.5$ mm, $L_4 = 9.5$ mm, $L_5 = 15.9$ mm, $L_6 = 45$ mm, $L_7 = 15.4$ mm, and $\theta = 26.5°$. A photograph of the fabricated sample is shown in Fig. 4. The simulated and measured $|S_{11}|$ of the proposed antenna are plotted in Fig. 5. The simulated results with the Ansoft HFSS agree reasonably well with the measured ones taken by the Agilent network analyzer E8363B. From the measured results, the resonance frequencies and -10 dB impendence bandwidths of the tri-band antenna are, respectively, 1.575 GHz and 1520-1610 MHz (5.7%), 2.4 GHz and 2270-2570 MHz (12.5%), and 5.2 GHz and 5090-6300 MHz (23.2%). Fig. 6 shows the simulated and measured radiation patterns of the proposed antenna. It was measured in an anechoic chamber at National Taiwan University of Science and Technology using the NSI-700S-90 scanner. The proposed antenna consistently shows quasi-omnidirectional radiation patterns in the *yz*-plane. The measured peak gains are 3.31, 3.8, and 2.04 dBi at the center frequencies, 1.575, 2.4 and 5.2 GHz, of the three bands. The measured radiation efficiencies are 67%, 74.4%, and 81.4%.

4. Conclusion

A compact tri-band printed monopole antenna for GPS L1 and 2.4/5-GHz WLAN bands has been presented and validated. Benefitting from the via-free configuration, the proposed antenna features the advantages of easy fabrication and low cost. The measured results demonstrate that the proposed tri-band monopole antenna provides good radiation characteristics at all three operation bands.

Acknowledgments

This work was supported by the National Science Council, R.O.C., under Grant 99-2628-E-011-001.

References

[1] Y. Zhou, C.-C. Chen and J. L. Volakis, "Dual band proximity-fed stacked patch antenna for tri-band GPS applications," *IEEE Trans. Antennas Propag.*, vol. 55, no. 1, pp. 220-223, Jan. 2007.

[2] J. Anguera, G. Font, C. Puente, C. Borja, and J. Soler, "Multifrequency microstrip patch antenna using multiple stacked elements," *IEEE Microw. Wireless Compon Lett.*, vol. 13, no. 3, pp.123-124, Mar. 2003.

[3] Y. Zhou, C.-C. Chen and J. L. Volakis , "Tri-band miniature GPS array with a single-fed CP antenna element," *IEEE Trans. AP-S, Int. Symp. Dig*. pp. 3049-3052, Jun. 2007.

[4] S. Liu and Q.-X Chu, "A novel dielectrically-loaded antenna for tri-band GPS applications," in *Proc. 38th Eur. Microw. Conf.*, pp. 1759-1762, Oct. 2008.

[5] A. Rennings, T. Liebig, S. Abielmona, C. Caloz and P. Waldow, "Tri-band and dual-polarized antenna based on composite right/left-handed transmission line," in *Proc. 37th Eur. Microw. Conf.*, pp. 720-723, Oct. 2007.
[6] M. Zhang, Z. Shen and C. Qian, "An inverted cavity-backed tri-band slot antenna," in *Proc. Asia-Pacific Microw. Conf.*, pp. 1-4, Dec. 2007.
[7] O. Luukkonen, A.O. Karilainen, J. Vehmas and S. A. Tretyakov, "A tri-band low-profile antenna based on a high-impedance surface," *IEEE Trans. AP-S, Int. Symp. Dig.* pp. 1-4, Jul. 2010.

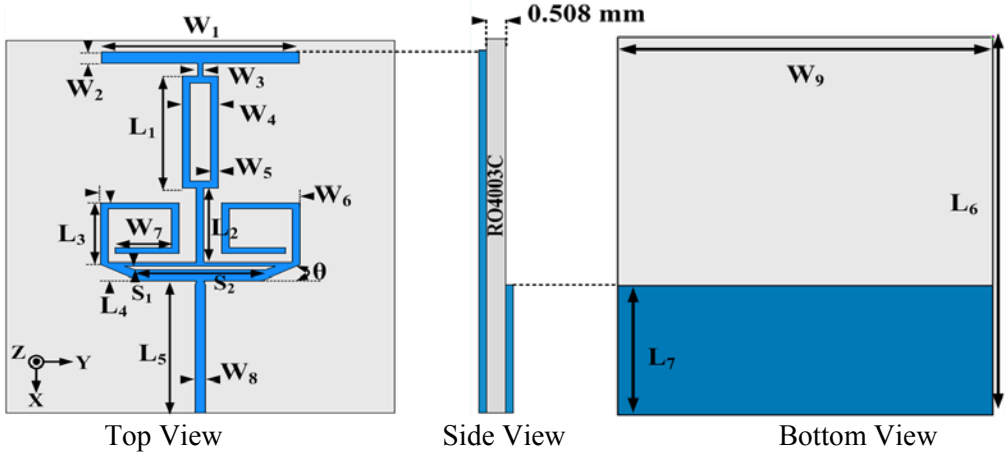

Figure 1: Geometry of the Proposed Antenna.

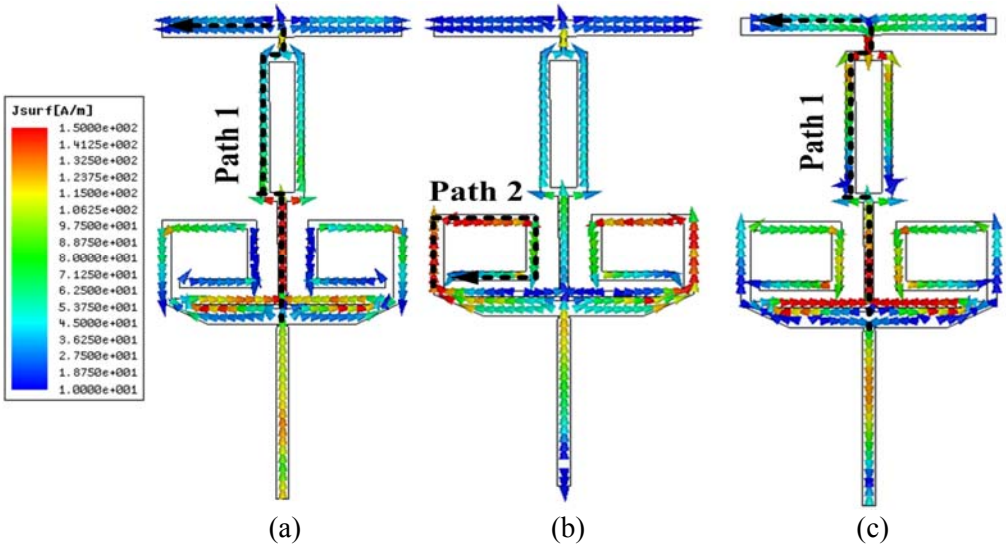

Figure 2: Current Distributions on the Antenna Surface at (a) 1.575, (b) 2.4, and (c) 5.2 GHz.

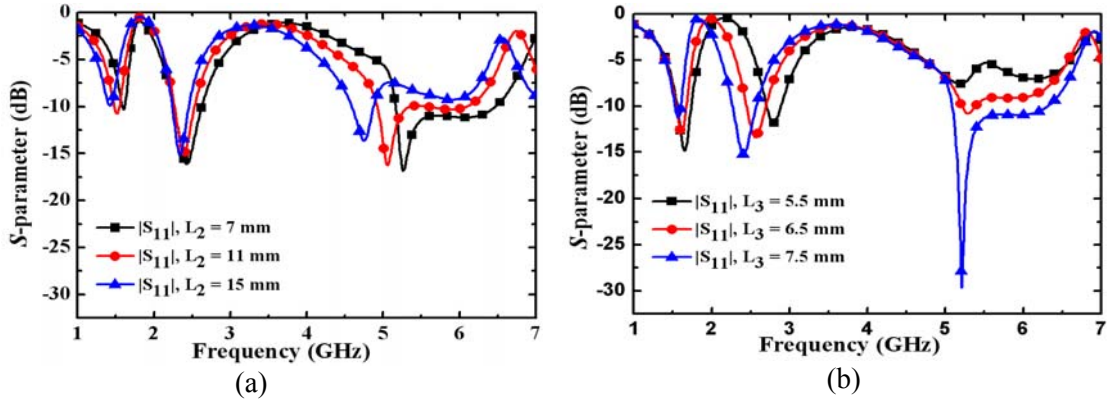

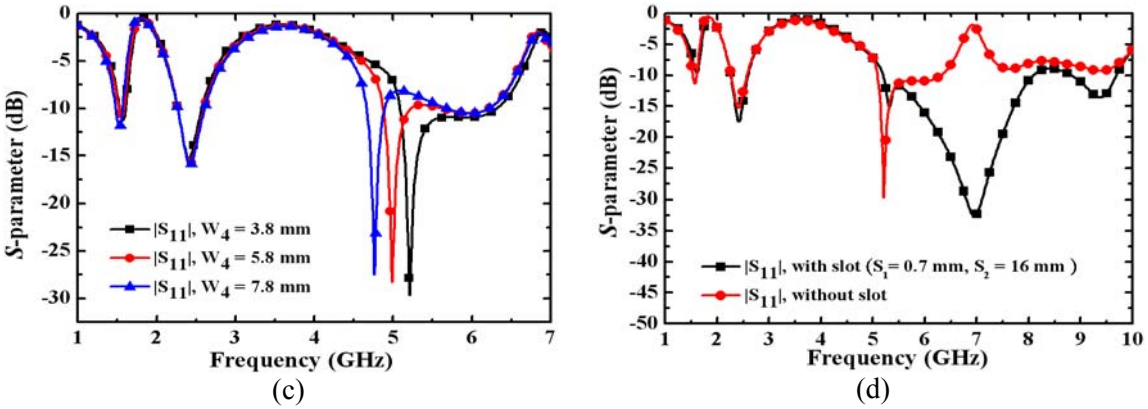

Figure 3: $|S_{11}|$ Responses with Respect to the Variations of (a) L_2, (b) L_3, (c) W_4, and (d) $S_1 \times S_2$.

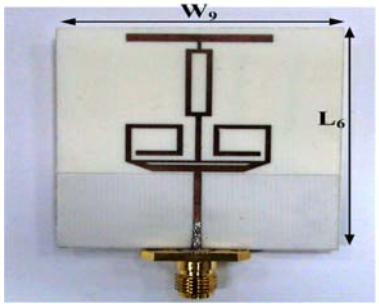

Figure 4: Photograph of the Fabricated Sample.

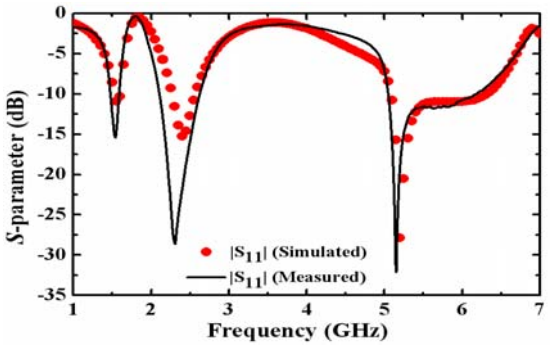

Figure 5: Simulated and Measured Antenna Reflection Coefficients.

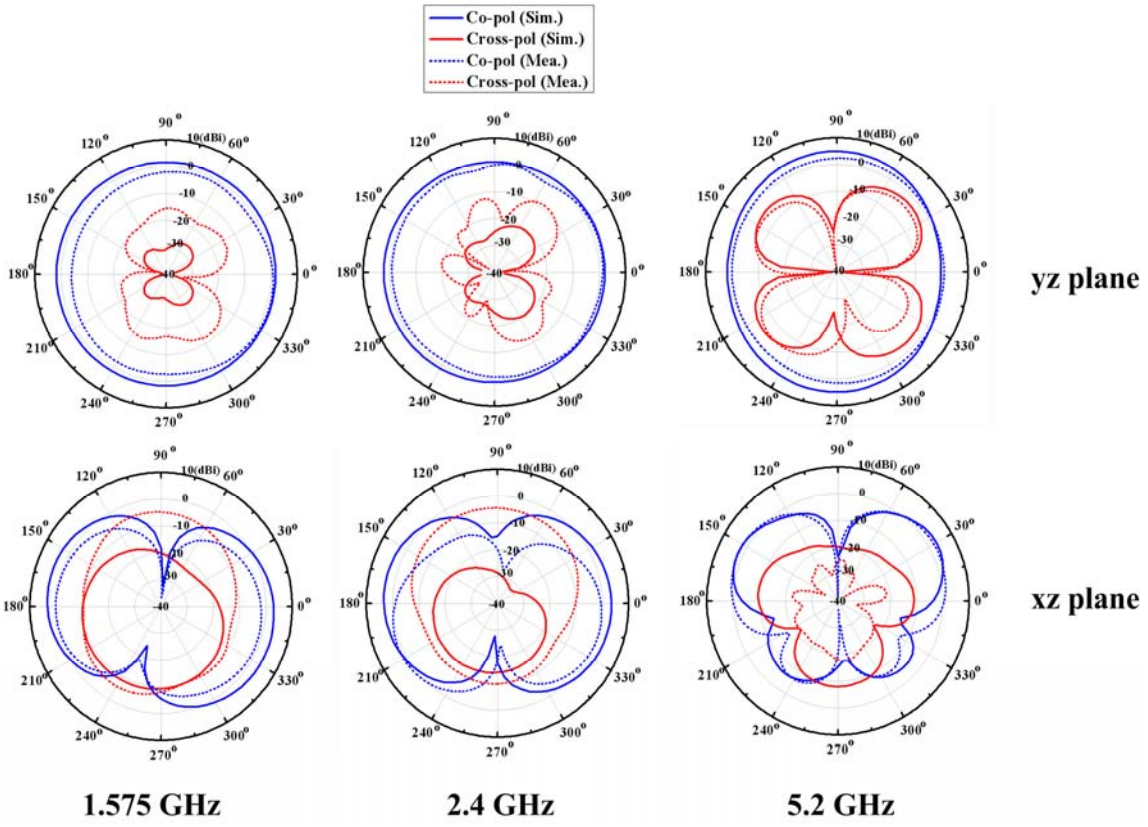

Figure 6: Simulated and Measured Radiation Patterns in the *xz* and *yz* planes.